Supplementary material to dataset of experimental estuaries

S1. Tabular overview of experimental dataset

Table S1. Number of available files for all experiments in the dataset. See Table S2 for more details about the relevant overhead orthomosaics. In agreement with the filenames, tidal cycles are provided in pseudocode of 5 digits.

Planform (Section S2)	lab No.	interval tidal cycles	dye conc.	# emulated tidal cycles	DEMs*	Masks	Orthomosaics				Water depth maps		Time-lapse
							DSLR	Overhead			Overhead		
								interval*	1Hz*	PIV	interval	1Hz	
S2.1 Control	057	20	3	03750	14	1	24	188			178		2
	075	20	4	04000	7	3	14	200	831		200	831	9
S2.2 Narrow	063	20	5**	19205	21	1	42	931	554	210	931	554	7
	063 Pilot 1		5	00020	2	1	4		277	210		277	2
	064	20	3	19000	9	1	20	946	1068	690	946	1069	10
S2.3 Widening −	059	20	3	13500	27	1	52	663		360	663		2
	060	20	4&5	15100	17	1	33	755			739		3
S2.4 Widening +	061	20	4	15017	14	1	28	750	396	400	750	396	7
	062	20	5	09000	15	1	30	450			437		2
S2.5 Planform 1	052	20	2	25000	56		74	1225			1193		2
	053	20	2	24000	41	1	82	1115			1093		2
	054	20	4	21000	21	1	43	1046		870	1029		2
	054 Pilot 1	1	2	01000	12	1	24	1000			995		2
	056	20	3	03000	18	1	34	150			138		2
	055	20	4	20000	13		25	1000			989		2
S2.6 Planform 2	076 Pilot 1	20	2	02000	3	1	6	100			99		2
	076	20	2	09000	9	1	18	449			450		2
	077	20	2	12709	9		18	635	1108	450	634	1108	11
	078	20	2	11500	5	1	10	548	554	430	546	554	7
S2.7 Rivers***	080		2		15	1	17	3851			3811		2
	081		2		10	1	8	2822			2809		2
Total				227801	338	20	606	18824	4788	3620	18630	4789	82

*For data available in both resolutions (25 mm and 5 mm), only the counts for the 5mm resolution are provided.

**Exp063 has a dye concentration of 5 mg/L for the interval imagery, and varying dye concentrations for the 1Hz imagery (Section S2.2.1).

***There is no periodic tilting of the facility for Exp080-081, so overhead imagery is collected every 60 seconds instead of intervals of tidal cycles.

Table S2. Overview showing the different overhead orthomosaics data, and which tidal cycles in the experiments they represent. In agreement with the filenames, tidal cycles are provided in pseudocode of 5 digits. Note that the *interval* and *1Hz* overhead orthomsaics have also been computed into water depth maps.

Planform (Section S2)	lab No.	interval	Available imagery			Missing imagery
			interval	1 Hz	PIV	
S2.1 Control	057	20	00000-03750			
	075	20	00007-04000	00000-00007, 03500-03507		
S2.2 Narrow	063	20	00000-19000	19000-19007, 19007-19014 19014-19021	19195-19205	
	063 Pilot 1			00000-00007	00010-00020	
	064	20	00026-19000	00000-00007, 12009-12019 12129-12139	00009-00019, 12000-12007 12239-12249	
S2.3 Widening −	059	20	00010-13500		00000-00010, 10160-10170	00055-00072 00300-00515
	060	20	00000-15100			
S2.4 Widening +	061	20	00017-15000	00004-00007, 15010-15017	00007-00017, 15000-15010	
	062	20	00000-09000			
S2.5 Planform 1	052	20	00000-25000			02000-02500
	053	20	00000-24000			06292-08000
	054	20	00022-21000		00001-00011, 11000-11015 11015-11030	00050-00070
	054 Pilot 1	1	00000-01000			
	056	20	00000-03000			
	055	20	00000-20000			
S2.6 Planform 2	076 Pilot 1	20	00000-02000			
	076	20	00000-09000			
	077	20	00000-12675	04000-04007, 04007-04014 12675-12682, 12682-12689	12689-12699, 12699-12709	
	078	20	00063-11011	00007-00014, 00014-00021	00021-00031, 00031-00041	

Table S1 provides the number of files in the dataset (Nota et al., 2026a) for all data types per experiment. For the data existing in both 25 mm and 5 mm resolution, only the counts of the 5 mm resolution are provided. These generally have the same count, but differences occur for the overhead interval orthomosaics, because some timesteps have not been processed as

the imagery was taken right after a dry bed laserscan and DSLR survey. This resulted in the setup not having enough water, and therefore orthomosaics representing shallower water depths than actually occur. These irrelevant timesteps (see the metadata file) have therefore been excluded from all timelapse videos, and partially from the 25 mm resolution orthomosiacs and water depth maps, hence there is not always exact correspondence between interval overhead orthomosaics and interval water depth maps.

The interval overhead orthomosaics typically start with the first tidal cycle in the experiment, in equal steps of the interval of 20 cycles (1 cycle for Exp054 Pilot 1). For a few experiments, the consistent interval is interrupted because of the exclusion of ranges of tidal cycles due to: (i) collection of 1Hz overhead imagery; (ii) collection of PIV overhead imagery; or (iii) missing overhead imagery due to oversight. Table S2 provides all ranges of tidal cycles of the different types of overhead orthomosaics that are available for the estuarine experiments in the dataset.

S2. Descriptive overview of experimental dataset

Here we briefly describe each experiment in the dataset, including general information, but with a main focus on particular information that may be relevant for any user of the dataset. We refrain from providing interpretations of these experiments. Daily information of each experiment can be found in the unrefined log text files in the dataset. Note that the log files occasionally mention acoustic elevation sensors, which can also be visible on the timelapses, and which are usually fixed at $x \approx 20$ m, therefore showing apparent high elevation values of the DEMs here that can be ignored (Fig. 1.f). These acoustic measurements are not included in this dataset because we often encountered issues with these sensors and calibrations. Instead, the water depth maps provide water depth data that are fully spatially and temporally covering, making the acoustic sensors redundant.

Furthermore, for the experiments with banks fixed by coarse sandpaper, it can occasionally be observed in the timelapses that sand disappears next to the dikes within the inactive bed. This is due to local bed erosion exposing the downward side of the sandpaper and allowing for seepage of sand from the inactive bed into the channel. Moreover, the timelapses can show floating foam and small grains, especially at the beginning of experiments. A final occasional observation in the timelapses is a reduced light intensity, which is caused by oversight of not setting the lighting to maximum intensity. When this happens, it has a limited effect on the predicted water depths, as the Random Forest models show low feature importance for color bands representing brightness (Nota et al., 2026b).

For all estuarine experiments (Sections S2.1-S2.6), the tidal cycle period is $T = 40$ s. See Tables S1-S2 for the number of data files and relevant ranges of overhead imagery. The complementary river experiments have a different setup, described in Section S2.7. For experiment numbers 052 until 062, we did not yet develop the spectrophotometry protocol (Nota et al., 2026b). The dye concentrations of these experiments were determined by finding the best fit from all Random Forest models (Nota et al., 2026b). Below we distinguish in subsections per planform, first providing the general setups of these planforms, and then discussing experiment-specific information. For each of these experiments, we present the first and final available interval overhead orthomosaics (Figs. S1-S20).

S2.1 Control runs without fixed banks

The control runs (lab numbers 057 & 075; Figs. S1-S2) consisted of an initial straight 80 cm-wide channel with a flat bed from $y \approx 1.1$ m until $y \approx 1.9$ m and from $x = 0$ m until $x \approx 18$ m. These experiments were conducted under asymmetric tidal cycles and banks were allowed to erode until the edge of the facility was nearly reached.

S2.1.1 Exp057 - Control run without fixed banks

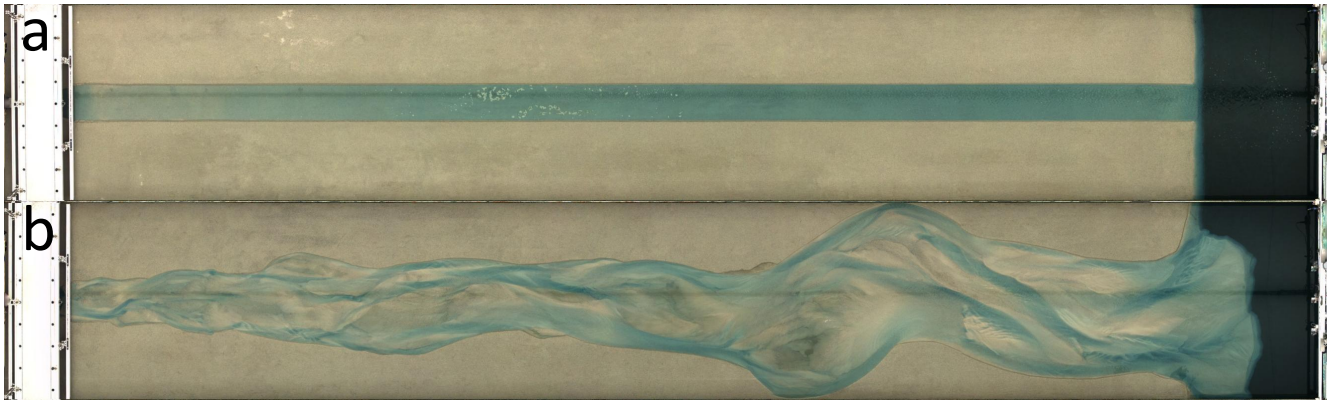

Figure S1. Interval overhead orthomosaics of Exp057 (5 mm resolution) at tidal cycles: (a) 00000; and (b) 03740.

Exp057 (Fig. S1) was conducted for a total of 03750 cycles. The optimal dye concentration was fitted to best match random forest classifier and regressor *Models 3*.

S2.1.2 Exp075 - Control run without fixed banks ***repeat***

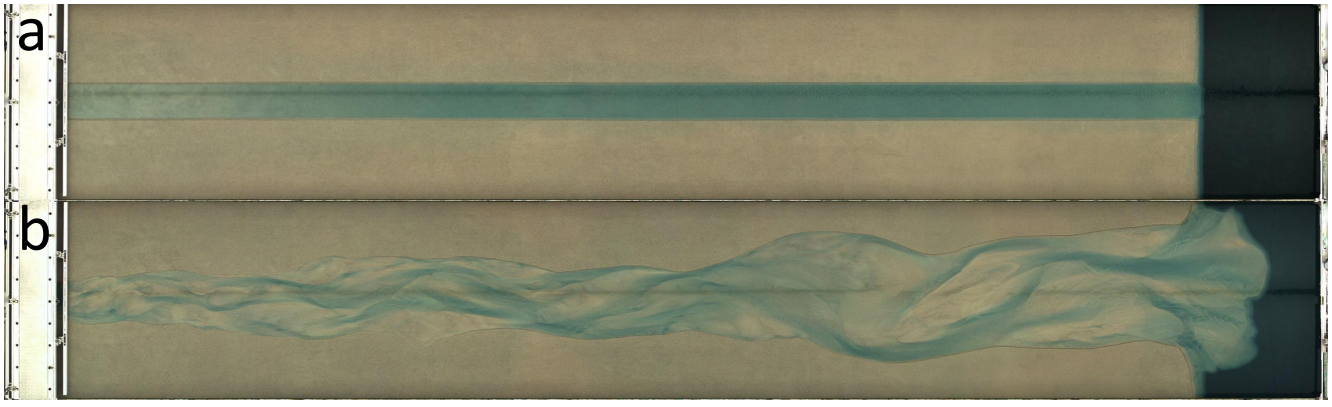

Figure S2. Interval overhead orthomosaics of Exp075 (5 mm resolution) at tidal cycles: (a) 00007; and (b) 03994.

Exp075 (Fig. S2) was a repeat experiment of Exp059 that was conducted for a total of 04000 cycles. The optimal dye concentration was maintained and daily measured to best match random forest classifier and regressor *Models 4*. The experiment

contains multiple masks because these had to be designed from the laserscan DEMs of the final timestep and for the timesteps at which the 1 Hz imagery was collected (Table S2), because the planform was not fixed and changed over time.

S2.2 Narrow fixed planform

The narrow fixed planform experiments (lab numbers 063-64; Figs. S3-S4) consisted of an initial straight 80 cm-wide channel with a flat bed from $y \approx 0.1$ m until $y \approx 0.9$ m and from $x = 0$ m until $x \approx 18$ m. These experiments were conducted under asymmetric tidal cycles and the banks were fixed with coarse sandpaper (also see Kleinhans et al., 2026).

S2.2.1 Exp063 - Narrow planform vertical fixed banks

Exp063 (Fig. S3) was an experiment conducted for 19205 cycles. The dye concentration was determined and maintained to best match random forest classifier and regressor *Models 5*. Prior to the experiment, the coarse sandpaper embankments were positioned vertically in the bed. This configuration of vertically placed embankments caused much more dike failures throughout the experiment than for any of the other experiments, leading to sand from the inactive bed leaking into the active channel from below, resulting in net sediment input. Moreover, from ∼9000 cycles onward, the upstream area got increasingly infested by biological pests, being visible as a dark brown color. The accuracy of the water depth maps at this location is uncertain, as such substrate has not been included in the training data of the machine learning models (Nota et al., 2026b, c). Of particular interest for Exp063 are the three sets of 1Hz overhead imagery and water depth maps at cycles 19000-19021 (Table S1). Before running these cycles and collecting the imagery, the dye concentration was recharged at 3.0 mg/L (19000-19007), 3.9 mg/L (19007-19014), and 5.15 mg/L (19014-19021).

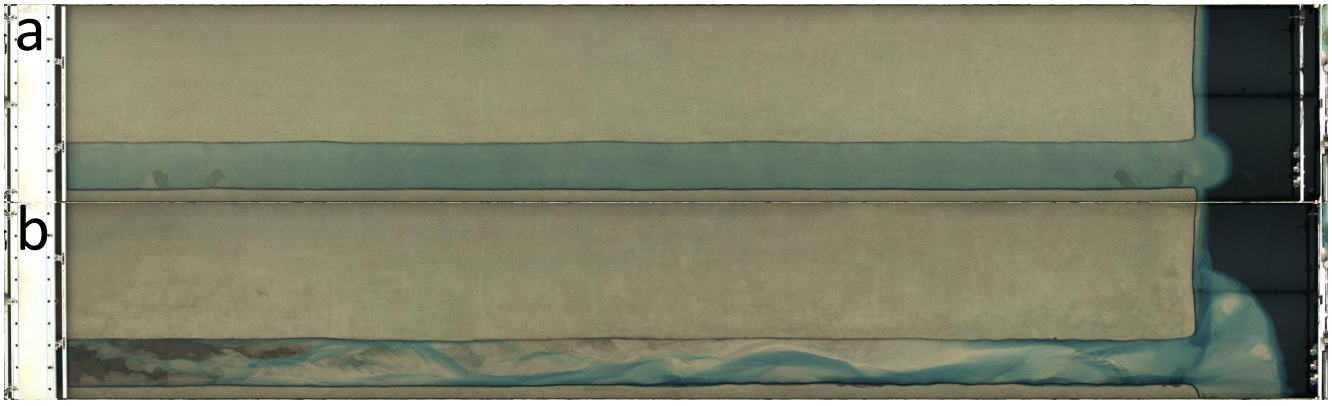

Figure S3. Interval overhead orthomosaics of Exp063 (5 mm resolution) at tidal cycles: (a) 00000; and (b) 18980.

S2.2.2 Exp063 Pilot 1 - Additional data to Exp063

Exp063 Pilot 1 was the initial attempt of Exp063, which failed early in the experiment because of a weir jam. Only relevant are: (i) the *PIV* overhead orthomosaics; and (ii) *1Hz* overhead orthomosaics and their derived water depths maps. Because of the smoothed initial bed, this data is representative for the initial condition of Exp063.

S2.2.3 Exp064 - Narrow planform inclined fixed banks

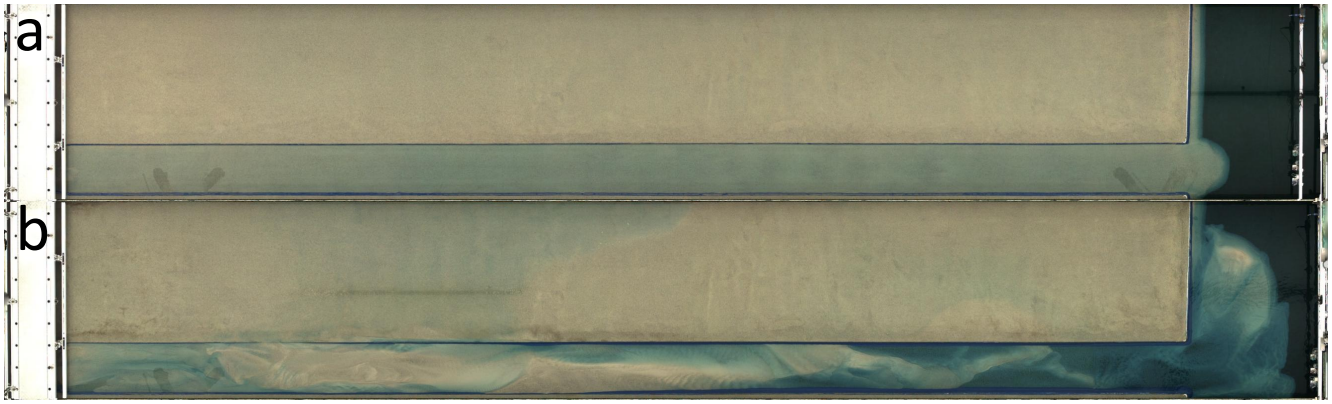

Figure S4. Interval overhead orthomosaics of Exp064 (5 mm resolution) at tidal cycles: (a) 00026; and (b) 18980.

Exp064 (Fig. S4) was an experiment conducted for 19000 cycles. The dye concentration was determined and maintained to best match random forest classifier and regressor *Models 3*. Exp064 had a similar setup as Exp063, but with steel-reinforced sandpaper banks that, moreover, were inclined at an angle of 45 degrees to test the effects of turbulence and scour depth near the banks. This planform was also used to collect the training and validation data for the Random Forest models (Nota et al., 2026b, c). As opposed to Exp063, this embankment configuration turned out to be sturdy and did not cause any problems. However, it is not straightforward to compare the effects of embankment inclination between Exp064 and Exp063, due to the extensive sand leakage in the latter. From $\sim$13000 cycles, a bar at $x \approx 8$ m starts to grow higher than the embankments, resulting in deposition of sand on the inactive bed. From $\sim$17000 cycles, increasing water levels from $x \approx 5$ m until $x \approx 8$ m resulted in flooding of the inactive bed.

S2.3 Seaward widening fixed planform narrow

The seaward widening fixed planform narrow experiments (lab numbers 059-060; Figs. S5-S6) consisted of a narrow river inlet of $\sim$0.2 m wide, with fixed embankments that straightly widen seaward to a width of $\sim$2 m at $x \approx 18$ m. These experiments were conducted under asymmetric tidal cycles and the banks were fixed with coarse sandpaper positioned vertically in the bed.

S2.3.1 Exp059 - Seaward widening fixed banks narrow

Exp059 (Fig. S5) was conducted for a total of 13500 cycles. The optimal dye concentration was fitted to best match random forest classifier and regressor *Models 3*.

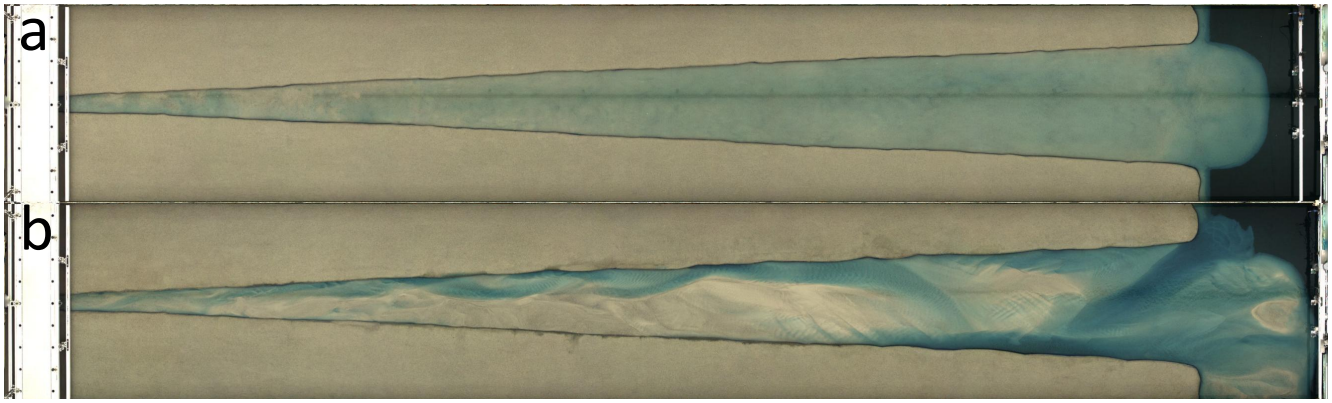

Figure S5. Interval overhead orthomosaics of Exp059 (5 mm resolution) at tidal cycles: (a) 00010; and (b) 13492.

S2.3.2 Exp060 - Seaward widening fixed banks narrow ***repeat***

Exp060 (Fig. S6) was a repeat experiment of Exp059 that was conducted for a total of 15100 cycles. The optimal dye concentration was fitted to best match random forest classifier and regressor *Models 4* up until cycle 09160, and *Models 5* for the cycles afterwards. For the first 100 cycles of the Exp060, the exposure settings of the cameras were set incorrectly, resulting in incorrectly processed orthomosaics and water depth maps for these cycles. From ∼07000 cycles, a bar at $x \approx 10$ m starts to grow higher than the embankments, resulting in deposition of sand on the inactive bed, as well as flooding. We are unsure why there is a sudden increase of dye concentration after cycle 09160, as there is nothing in the log text file that mentions it.

Figure S6. Interval overhead orthomosaics of Exp060 (5 mm resolution) at tidal cycles: (a) 00100; and (b) 15080.

S2.4 Seaward widening fixed planform wide

The seaward widening fixed planform narrow experiments (lab numbers 061-062; Figs. S7-S8) consisted of narrow river inlet of ∼0.2 m wide, with fixed embankments that straightly widen seaward to a width of ∼3 m at $x \approx 18$ m. These experiments were conducted under asymmetric tidal cycles and the banks were fixed with coarse sandpaper positioned vertically in the bed.

S2.4.1 Exp061 - Seaward widening fixed banks wide

Exp061 (Fig. S7) was conducted for a total of 15017 cycles. The optimal dye concentration was fitted to best match random forest classifier and regressor *Models 4*. There was some occasional minor flooding over the inactive bed.

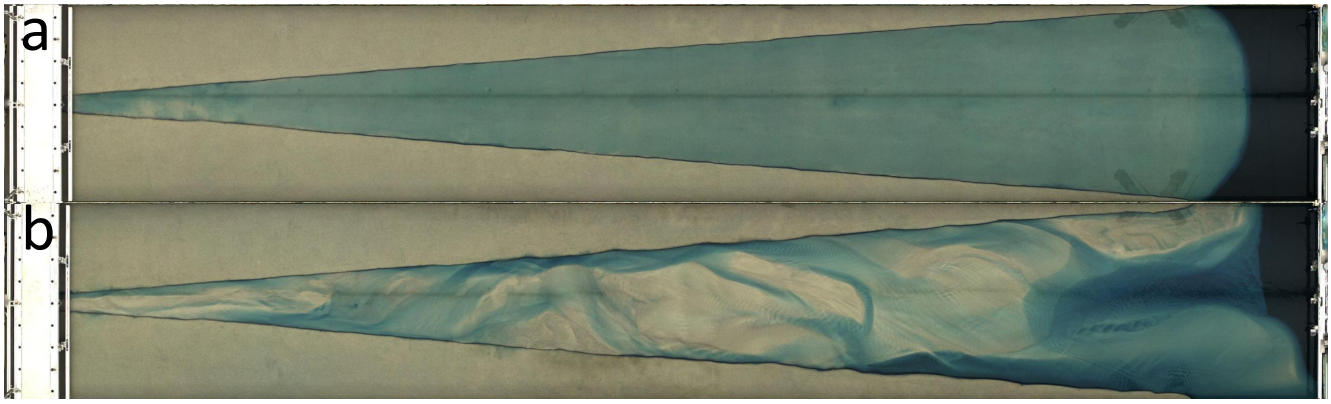

Figure S7. Interval overhead orthomosaics of Exp061 (5 mm resolution) at tidal cycles: (a) 00017; and (b) 14997.

S2.4.2 Exp062 - Seaward widening fixed banks wide ***repeat***

Exp062 (Fig. S8) was a repeat experiment of Exp061 and was conducted for a total of 09000 cycles. The optimal dye concentration was fitted to best match random forest classifier and regressor *Models 5*.

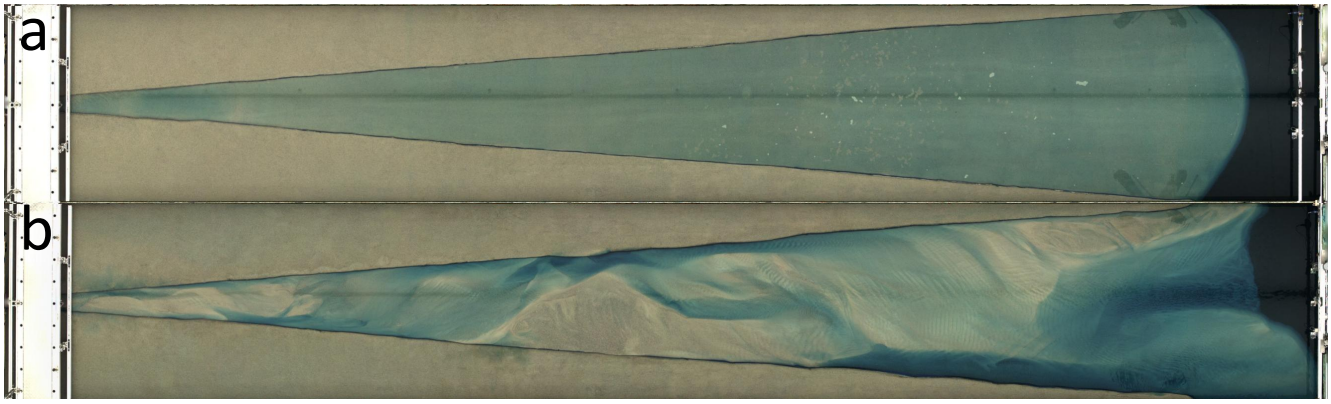

Figure S8. Interval overhead orthomosaics of Exp062 (5 mm resolution) at tidal cycles: (a) 00000; and (b) 08980.

S2.5 Naturally formed fixed planform 1: perturbations on initial conditions

The Naturally formed fixed planform 1 experiments (lab numbers 052-056; S9-S14) consist of a planform that was initially allowed to naturally form (as for the control runs Exp057 and Exp075) before being fixed with coarse sandpaper. Accordingly, this is a naturally formed planform, as opposed to Figs. S3-S8. The experiments in this subsection either have an initial flat bed, or initial perturbations compared to an initial flat bed. These experiments were conducted under asymmetric tidal cycles and the banks were fixed with coarse sandpaper positioned vertically in the bed.

S2.5.1 Exp052 - Naturally formed fixed planform 1

Exp052 (Fig. S9) was conducted for a total of 25000 cycles. The optimal dye concentration was fitted to best match random forest classifier and regressor *Models 2*. The initial condition of Exp052 consisted of an initial straight 80 cm-wide channel with a flat bed from $y \approx 1.1$ m until $y \approx 1.9$ m and from $x = 0$ m until $x \approx 18$ m (the same as the control runs; Section S2.1). The banks were allowed to naturally develop for 02000 cycles, after which the banks were fixed by positioning the coarse sandpaper $\sim$5 cm from the banks into the inactive bed, in order not to disturb the morphology. We refer to this planform as Naturally formed fixed planform 1, which was maintained throughout Experiments 052-056. Moreover, from $\sim$10000 cycles onward, a persistent bar between $x \approx 5$ m and $x \approx 7$ m got increasingly infested by biological pests, being visible as a dark brown color. The accuracy of the water depth maps at this location is uncertain, as such substrate has not been included in the training data of the machine learning models (Nota et al., 2026b, c). Between $\sim$16000 and $\sim$17000 tidal cycles, an oversight in refilling water at the reservoir caused the dye to nearly completely dilute. After $\sim$17000 cycles, dye was added again and fitted to best match random forest classifier and regressor *Models 2*. From $\sim$22500 cycles, a bar at $x \approx 10$ m started to grow higher than the embankments, resulting in deposition of sand on the inactive bed. Additionally, Exp052 contains several DEMs from laserscans that have been conducted under wet conditions, under the same conditions as the wet DSLR orthomosaics.

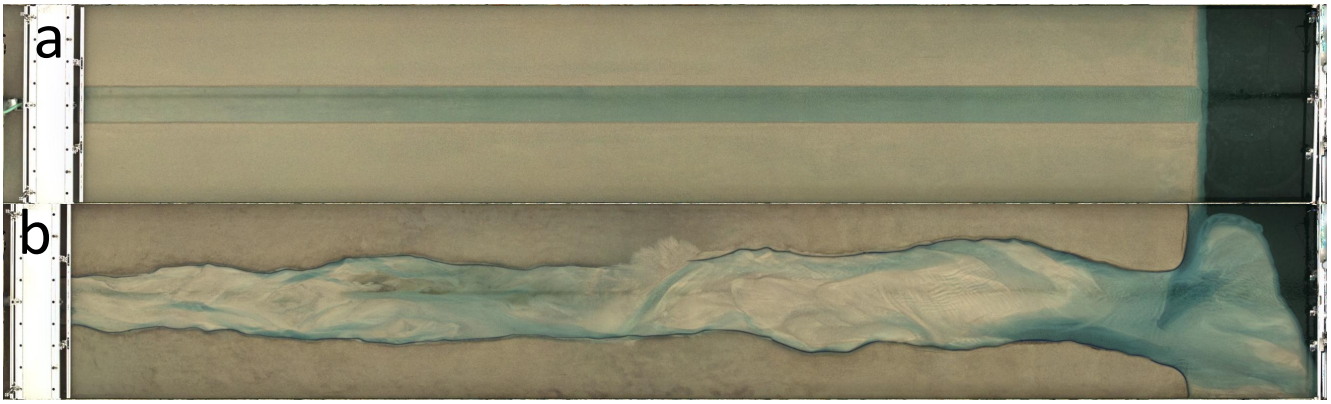

Figure S9. Interval overhead orthomosaics of Exp052 (5 mm resolution) at tidal cycles: (a) 00000; and (b) 24980.

S2.5.2 Exp053 - Naturally formed fixed planform 1 flat bed

Exp053 (Fig. S10) was conducted for a total of 24000 cycles. The optimal dye concentration was fitted to best match random forest classifier and regressor *Models 2*. The initial condition of Exp053 consisted of Naturally formed fixed planform 1 and a smoothed bed. The initial delta elevation from $x > 18$ m was slightly higher than the rest of the bed.

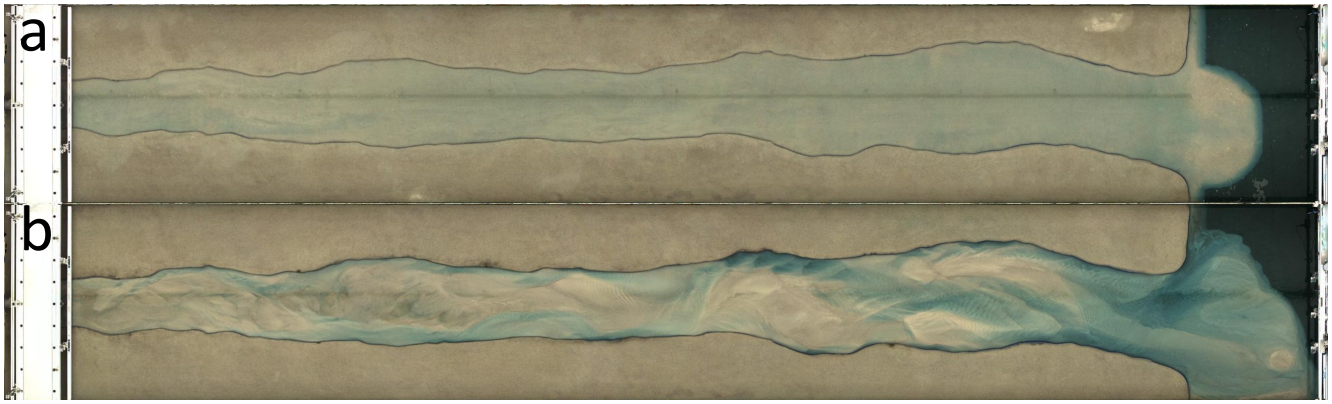

Figure S10. Interval overhead orthomosaics of Exp053 (5 mm resolution) at tidal cycles: (a) 00000; and (b) 23988.

S2.5.3 Exp054 - Naturally formed fixed planform 1 flat bed ***repeat***

Exp054 (Fig. S11) was a repeat experiment of Exp053 that was conducted for a total of 21000 cycles. The optimal dye concentration was fitted to best match random forest classifier and regressor *Models 4*. The predominant difference in initial condition from Exp053 is that for Exp054 the delta at $x > 18$ m was smoothed to match the elevation of the channel bed. From $\sim$16000 cycles, a bar at $x \approx 8$ m started to grow higher than the embankments, resulting in deposition of sand on the inactive bed.

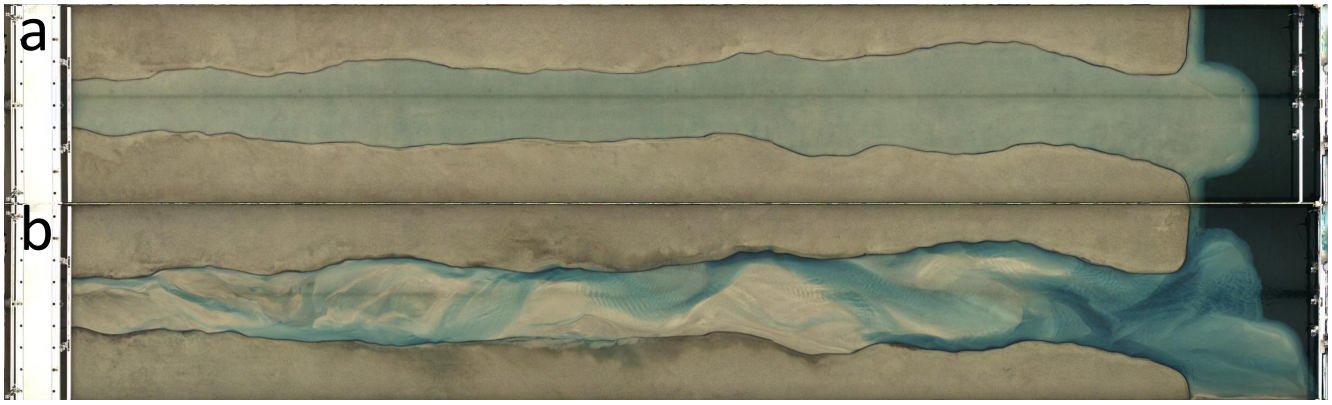

Figure S11. Interval overhead orthomosaics of Exp054 (5 mm resolution) at tidal cycles: (a) 00022; and (b) 20982.

S2.5.4 Exp054 Pilot 1 - Naturally formed fixed planform 1 small perturbations

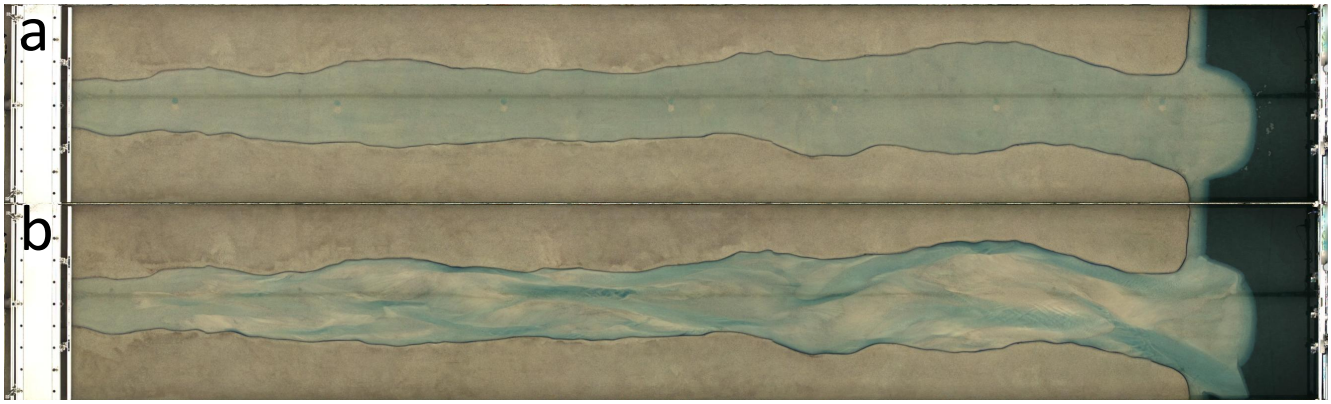

Figure S12. Interval overhead orthomosaics of Exp054 Pilot 1 (5 mm resolution) at tidal cycles: (a) 00000; and (b) 00999.

Exp054 Pilot 1 (Fig. S12) was conducted for a total of 01000 cycles. The optimal dye concentration was fitted to best match random forest classifier and regressor *Models 2*. The initial condition of Exp054 Pilot 1 consisted of Naturally formed fixed planform 1 and a smoothed bed, in which seven minor perturbations were applied. These perturbations were equally spaced from each other at $y \approx 1.5$ m between $x \approx 2.5$ m and $x \approx 17.5$ m in steps of 2.5 m. These perturbations had the shape of a small bump at $y \approx 1.45$ m a small hole at $y \approx 1.55$ m, both with a diameter of $\sim$0.1 m. Exp054 Pilot 1 has an interval of 1 for the processed interval overhead imagery and water depth maps, and is therefore the only experiment without an interval of 20 (Table S1). Exp054 Pilot 1 is also referred to as the *Test time series* in Nota et al. (2026d). The online available dataset of this study also contains all raw sensor files for this experiment (Nota et al., 2025).

S2.5.5 Exp056 - Naturally formed fixed planform 1 large perturbations

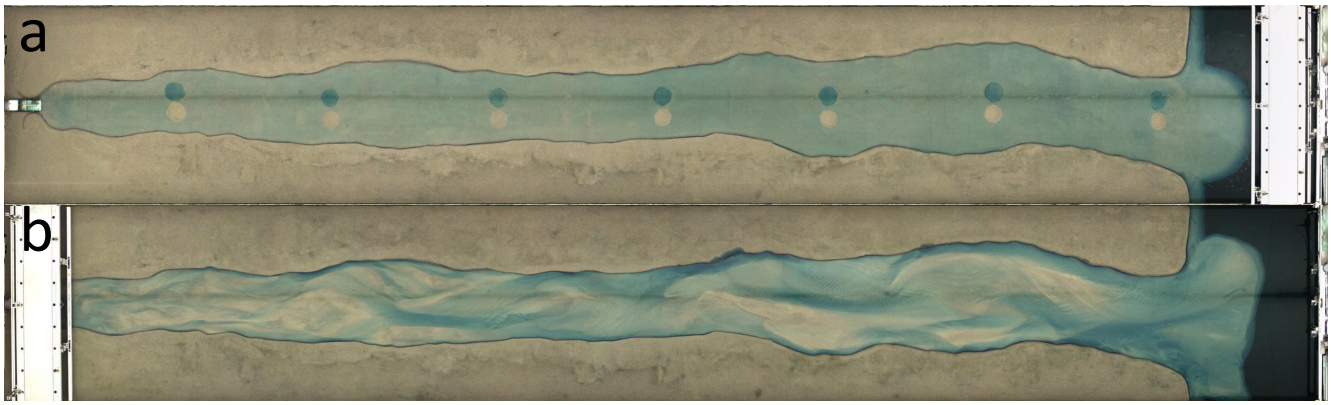

Figure S13. Interval overhead orthomosaics of Exp056 (5 mm resolution) at tidal cycles: (a) 00000; and (b) 02980.

Exp056 (Fig. S13) was conducted for a total of 03000 cycles. The optimal dye concentration was fitted to best match random forest classifier and regressor *Models 3*. The initial condition of Exp056 is comparable to Exp054 Pilot 1, and consisted of Naturally formed fixed planform 1 and a smoothed bed, in which seven perturbations were applied, equally spaced from each other at $y \approx 1.5$ m between $x \approx 2.5$ m and $x \approx 17.5$ m in steps of 2.5 m. The difference with Exp054 Pilot 1 is that the perturbations of Exp056 perturbations were notably larger, with the bump at $y \approx 1.35$ m hole at $y \approx 1.65$ m, both with a diameter of $\sim$0.3 m. Due to an oversight, the supporting cart was positioned on the far sea side for first 50 cycles (Fig. S13.a).

S2.5.6 Exp055 - Naturally formed fixed planform 1 reversed initial conditions

Exp055 (Fig. S14) was conducted for a total of 20000 cycles. The optimal dye concentration was fitted to best match random forest classifier and regressor *Models 4*. The initial condition of Exp055 was inspired by interpretations of the morphological developments over the longer timescales of Experiments 052-054 (Sections S2.5.1-S2.5.3). In these earlier experiments, we suspected topographic forcing of certain bars, channels and scours, of which the positions appeared repeatable between the experiments, especially for the downstream half of the flume (Figs. S9.b, S10.b & S11.b). Accordingly, for the initial setup of Exp055 we imposed a morphology from $x > 10$ m that was a loose interpretation of the reversed likely channel-bar positions for the given topographic forcing for planform 1. We did this by digging channels and scours where previously bars emerged, and constructing bars in areas that were previously dominated by channels and scours. At the mouth at $x \approx 18$ m, we built 10 sand castles. At the upstream area ($x < 10$ m), we did not observe any clear forcing patterns from the earlier experiments. Therefore, in this section we imposed a random morphology of a dredged meandering and anastomosing channel pattern surrounded by sand crabs and sand fish made from sand toys, finalized with some sand graffiti (Fig. S14.a). For cycles 02000-04000, the exposure settings of the cameras were set incorrectly, resulting in incorrectly processed orthomosaics and water depth maps for these cycles. From $\sim$13500 cycles, a bar at $x \approx 9$ m started to grow higher than the embankments, resulting in deposition of sand on the inactive bed, as well as flooding. For the final 1000 cycles, there was significant seepage of sand from the inactive bed into the active channel.

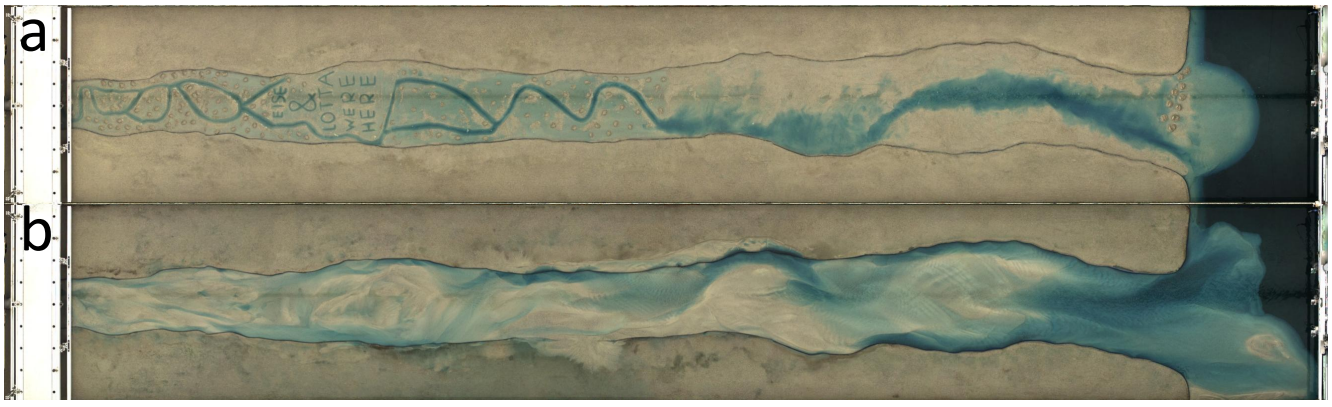

Figure S14. Interval overhead orthomosaics of Exp055 (5 mm resolution) at tidal cycles: (a) 00000; and (b) 19980.

S2.6 Naturally formed fixed planform 2: tidal symmetry

Similar to the previous planform, the Naturally formed fixed planform 2 experiments (lab numbers 076-078; S15-S18) consist of a planform that was initially allowed to naturally form before being fixed with coarse sandpaper. The experiments in this subsection all have an initial flat bed. The banks were fixed with coarse sandpaper positioned vertically in the bed. Unlike initial morphological perturbations of planform 2, the experiments for planform 2 were designed to observe the effects of fixed perturbations of tidal settings. Accordingly, unlike all previous experiments, this final set of experiments is not solely conducted under asymmetric tidal settings, but also symmetric tidal settings.

S2.6.1 Exp076 Pilot 1 - Natural formation of planform 2

Exp076 Pilot 1 (Fig. S15) was conducted for a total of 02000 cycles. The dye concentration was determined and maintained to best match random forest classifier and regressor *Models 2*. The initial condition of Exp076 Pilot 1 consisted of an initial straight 80 cm-wide channel with a flat bed from $y \approx 1.1$ m until $y \approx 1.9$ m and from $x = 0$ m until $x \approx 18$ m (the same as the control runs and experiment 052; Sections S2.1 & S2.5.1). At the end of the experiment, the banks were fixed by positioning the coarse sandpaper $\sim$5 cm from the banks into the inactive bed. Unlike for Exp052, we made no effort to preserve the bed morphology when fixing the banks, hence the end of this pilot experiment. We refer to this planform as Naturally formed fixed planform 2, which was maintained throughout Experiments 076-078.

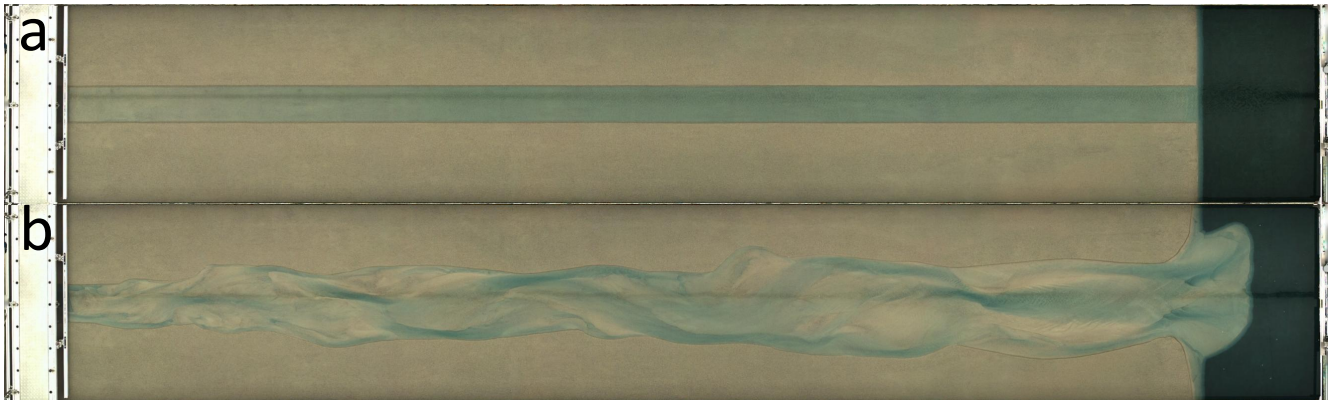

Figure S15. Interval overhead orthomosaics of Exp076 Pilot 1 (5 mm resolution) at tidal cycles: (a) 00000; and (b) 01980.

S2.6.2 Exp076 - Naturally formed fixed planform 2 asymmetric tide

Exp076 (Fig. S16) was conducted for a total of 09000 cycles. The dye concentration was determined and maintained to best match random forest classifier and regressor *Models 2*. The initial condition of Exp076 consisted of Naturally formed fixed planform 2 and a smoothed bed. Asymmetric tide was applied to the full experiment.

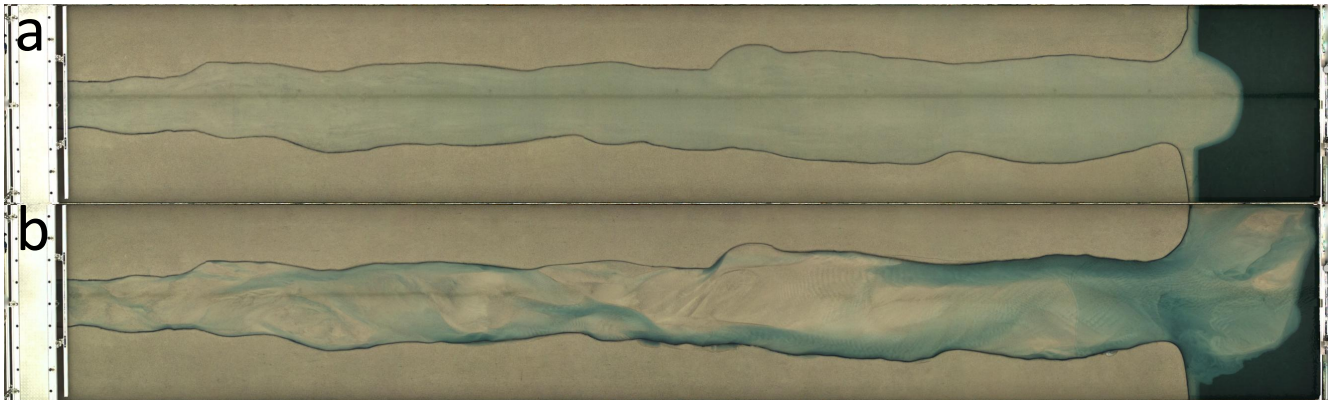

Figure S16. Interval overhead orthomosaics of Exp076 (5 mm resolution) at tidal cycles: (a) 00000; and (b) 08980.

S2.6.3 Exp077 - Naturally formed fixed planform 2 asymmetric & symmetric tide

Exp077 (Fig. S17) was conducted for a total of 12709 cycles. The dye concentration was determined and maintained to best match random forest classifier and regressor *Models 2*. The initial condition of Exp076 consisted of Naturally formed fixed planform 1 and a smoothed bed. Asymmetric tide was applied during the following ranges of cycles: 00000-04007; and 12682-12699. Symmetric tide was applied during the following ranges of cycles: 04007-12682; and 12699-12709. See Table S2 which types of overhead imagery were collected during these ranges. At 02000 cycles, a dike repair effort notably reduced the size of a bend at $x \approx 11$ m, hence the mask applied to Exp077 is derived from Exp078.

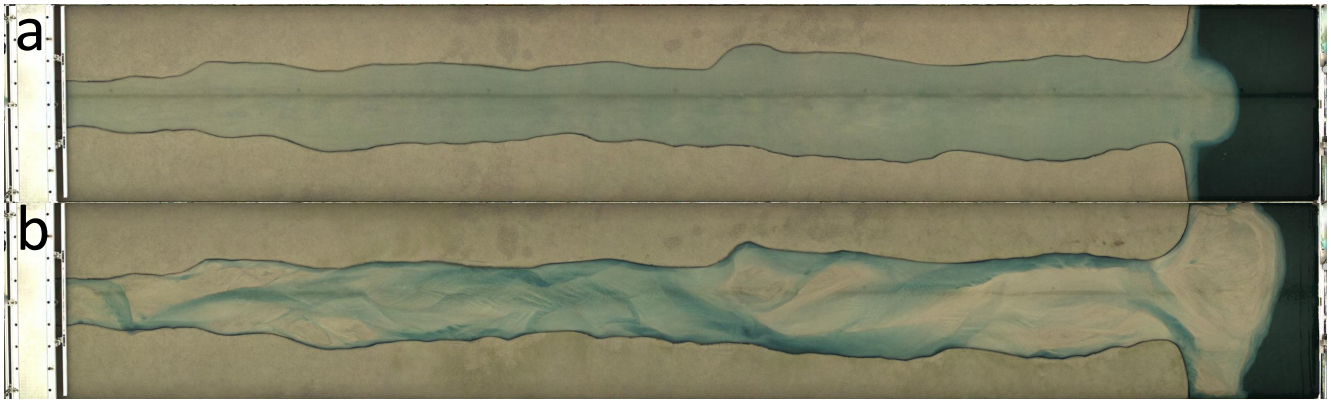

Figure S17. Interval overhead orthomosaics of Exp077 (5 mm resolution) at tidal cycles: (a) 00000; and (b) 12754.

S2.6.4 Exp078 - Naturally formed fixed planform 2 symmetric tide

Exp078 (Fig. S18) was conducted for a total of 11500 cycles. The dye concentration was determined and maintained to best match random forest classifier and regressor *Models 2*. The initial condition of Exp076 consisted of Naturally formed fixed planform 1 and a smoothed bed. Asymmetric tide was applied during the following range of cycles: 00014-00031. Symmetric

tide was applied during the following ranges of cycles: 00000-00014; and 00014-11500. Table S2 indicates which types of overhead imagery were collected during these ranges. Accordingly asymmetric tide was only applied to collect *1Hz* and *PIV* overhead imagery for the initial flat bed morphology, so practically the full morphological development of Exp078 occurred under symmetric tidal settings. For the cycles 11011-11500, interval overhead imagery was not stored as there was no local storage available anymore.

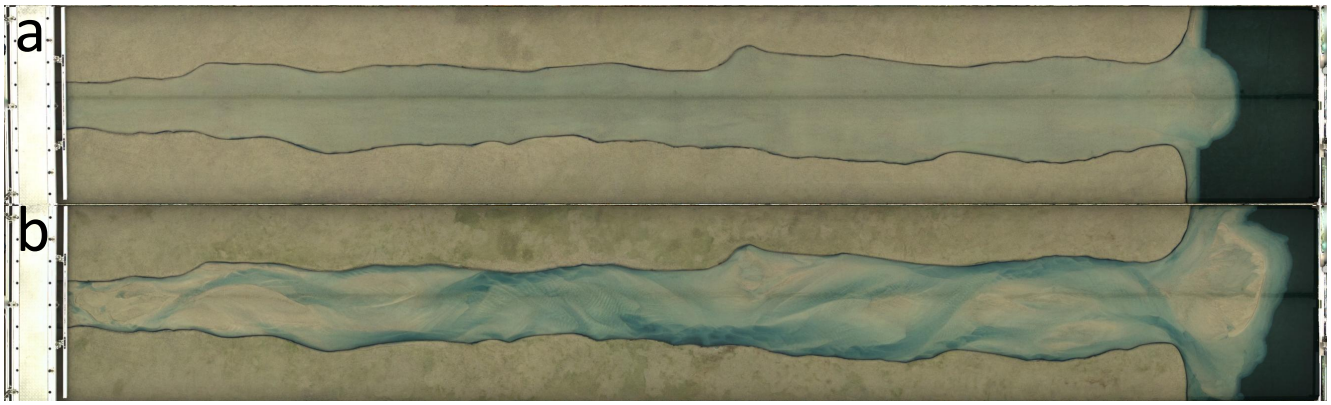

Figure S18. Interval overhead orthomosaics of Exp078 (5 mm resolution) at tidal cycles: (a) 00063; and (b) 11003.

S2.7 Complementary river experiments

We decided to conduct and include two complementary river experiments within the facility, because: (i) our improved data processing methods (Nota et al., 2026b, d) allow for new opportunities of quantitative research for experimental rivers; and (ii) these complementary experiments allow for research on comparability and scalability between both types of scale experiments.

The setups of complementary river experiments were inspired by previous studies (Van Dijk et al., 2012; Van de Lageweg et al., 2016), with an initial $\sim$0.18 m wide straight channel. The setups differed from the estuarine experiments as follows. First, there was no periodic tilting of the facility, but a fixed slope of 0.01. Accordingly, overhead imagery was not collected at set intervals of tidal cycles. Instead, the cameras were triggered every 60 seconds. Second, the river inlet was not fixed, but had a transverse movement at a rate of $\sim$10 mm/hr. Third, the wave maker was continuously generating waves during the full experiments, effectively inhibiting excessive delta growth. Fourth, sediment feeders were installed at the river inlet, providing a continuous supply of sediments throughout the experiments, preventing excessive upstream erosion. For Exp080, the sediment feed involved the same sand as in all experimental setups, at a rate of $\sim$0.2 L/hr. For Exp081, there was additional sediment feed of crushed walnut shell, which acts as a scalable cohesive material that deposits on shallow bars, and which has been proven to be crucial for the formation of meandering rivers in such experimental setups (Van de Lageweg et al., 2016). This crushed walnut shell was released into the river inlet while suspended in water at a rate of $\sim$1 L/hr. The crushed walnut shell has a density of 1350 kg/m^3 and a median grain size of $\sim$1.5 mm. Both experiments do not have fixed banks with coarse sand paper.

S2.7.1 Exp080 - Braiding river

Exp080 (Fig. S19) was conducted for a total of 3851 minutes. The dye concentration was determined and maintained to best match random forest classifier and regressor *Models 2*.

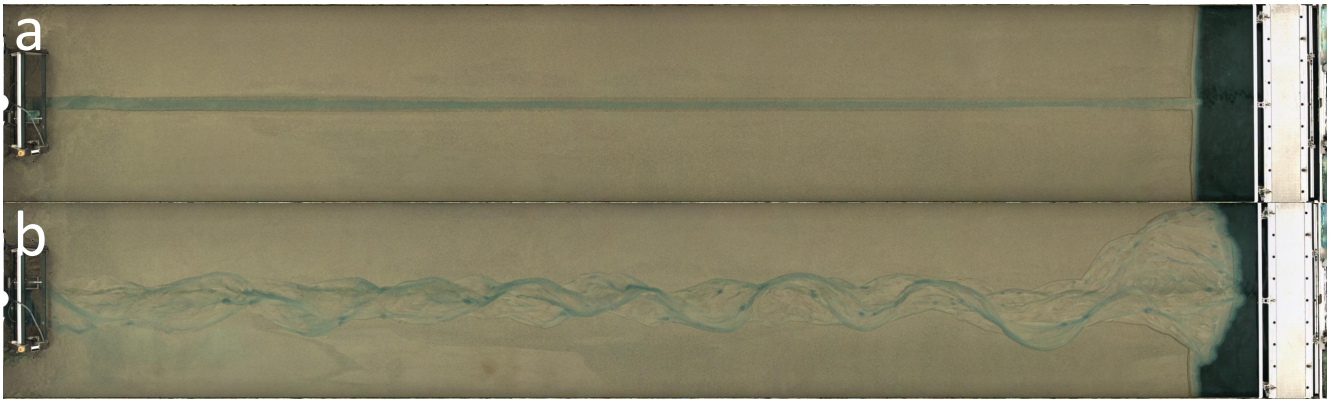

Figure S19. Overhead orthomosaics of Exp080 (5 mm resolution) at minutes: (a) 00004; and (b) 03850.

S2.7.1 Exp081 - Meandering river

Exp081 (Fig. S20) was conducted for a total of 2822 minutes. The dye concentration was determined and maintained to best match random forest classifier and regressor *Models 2*. Early on in the experiment, we observed overbank flooding in the upstream area, at $x \approx 2$ m, and after 1500 minutes at $x \approx 5$ m. For both occasions, we elevated the banks with a broad sand dike to force the flow back into the channel. Note that the random forest models were only trained on sandy substrate (Nota et al., 2026b, c), and not the walnut shell (Fig. S20.b). In the water depth maps we observe that the bars covered with walnut shell are predominantly predicted dry, but that the main channel and a few tributary channels are correctly identified wet. So the water depth maps of Exp081 are suitable for identifying channel network and sinuosity throughout the experiment.

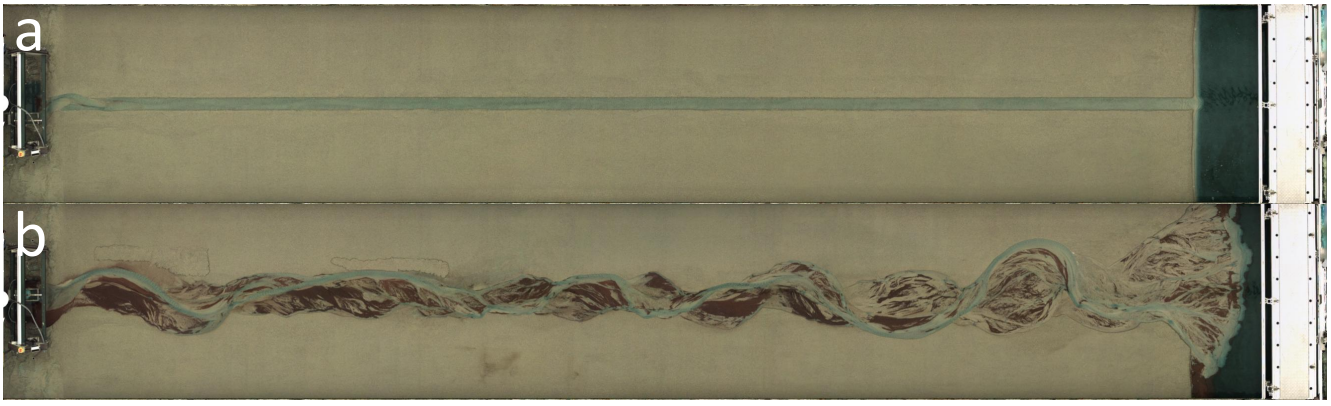

Figure S20. Overhead orthomosaics of Exp081 (5 mm resolution) at minutes: (a) 00002; and (b) 02821.

S3. Governing equations and numerical model XBeach

Here we briefly describe our effort to numerically model the estuarine experiments of the Metronome facility in XBeach, which is still ongoing work (available at https://github.com/saeb-faraji-gargari/Xbeach_dev_Moving_boundary/tree/20240110_XBeach_v4_20251114). XBeach is a depth-averaged two-dimensional horizontal (2DH) model for water flow, waves, sediment transport and morphological changes, specifically for tidal systems (Roelvink et al., 2009, 2010; McCall et al., 2022; Smit et al., 2010). So far, we have focused our modelling efforts only on hydrodynamic, which is simulated in XBeach following McCall et al. (2022).

The bed tilting effect is accounted for in the continuity (mass conservation) equation through the term $\partial z_b/\partial t$ (Eq.S1). The conservative form of the depth-averaged shallow water equations for mass and momentum conservation is discretized and solved to simulate the flow as follows:

$$\frac{\partial \eta}{\partial t} - \frac{\partial z_b}{\partial t} + \frac{\partial hu}{\partial x} + \frac{\partial hv}{\partial y} = 0 \tag{S1}$$

$$\frac{\partial u}{\partial t} + u\frac{\partial u}{\partial x} + v\frac{\partial u}{\partial y} - f_c v - \nu_h \left(\frac{\partial^2 u}{\partial x^2} + \frac{\partial^2 u}{\partial y^2} \right) = \frac{\tau_{sx}}{\rho h} - \frac{\tau_{bx}}{\rho h} - g\frac{\partial \eta}{\partial x} \tag{S2}$$

$$\frac{\partial v}{\partial t} + u\frac{\partial v}{\partial x} + v\frac{\partial v}{\partial y} + f_c u - \nu_h \left(\frac{\partial^2 v}{\partial x^2} + \frac{\partial^2 v}{\partial y^2} \right) = \frac{\tau_{sy}}{\rho h} - \frac{\tau_{by}}{\rho h} - g\frac{\partial \eta}{\partial y} \tag{S3}$$

where η is the water surface elevation, h is the water depth, f_c is the Coriolis parameter, which is neglected because the spatial scale of the experimental setup is too small for Coriolis effects to be significant. τ_{bx} and τ_{by} are the bed shear stresses, which here is calculated based on the Chezy coefficient (McCall et al., 2022). g is the scalar gravitational acceleration (9.81 m/s^2). ν_h is the horizontal viscosity. τ_{sx} and τ_{sy} represent the wind shear stresses, which are neglected in our model. It is worth noting that wave-induced, and vegetation stresses can also be included on the right-hand side of the momentum equation, which requires additional closure equations to compute their effects in XBeach (McCall et al., 2022; Roelvink et al., 2010). However, since this study focuses only on hydrodynamic effects, we neglect these contributions and therefore exclude them from the momentum equations.

The bed elevation z_b is defined as

$$z_b = z_{b0} + z_{tilt} \tag{S4}$$

where z_{b0} is the initial bed bathymetry function (i.e., $z_b(t = 0, x)$) and z_{tilt} is the Metronome tilting function defined in Eq. 1 (Section 2; see also Fig. S21.a for tilt movement at $x = 0$ m). So far, we have ignored bed morphology changes; hence, z_{b0} is assumed to be static in time.

$\partial z_b/\partial t$ is implemented in Eq. S1 as

$$\frac{\partial z_b}{\partial t} = \left(\frac{\frac{L}{2} - (x - x_0)}{\frac{L}{2}}\right)\left(-a_1 \frac{2\pi}{T}\sin\left(\frac{2\pi(t-t_s)}{T} - \phi_1\right) - a_2 \frac{2N\pi}{T}\sin\left(\frac{2N\pi(t-t_s)}{T} - \phi_2\right)\right) \tag{S5}$$

See also Fig. S21.b for this tilt derivative at $x = 0$ m. Note that Eq. S5 contains two phase shift terms (ϕ_1, ϕ_2), instead of the single phase shift in Eq. 1 (Section 2). These two phase shifts are included for the purpose of model flexibility. Accordingly, Table S3 provides an updated version of Table 1 (Section 2), to match with all the XBeach input parameters.

Table S3. Overview of the fixed parameters for asymmetric and symmetric tidal settings as implemented in XBeach

Parameter	Asymmetric tide	Symmetric tide
a_1 (m)	0.075	0.075
a_2 (m)	0.015	0
t_s (s)	1.192	0
N (-)	2	1
ϕ_1 (rad)	$\pi/2$	0
ϕ_2 (rad)	0	0
L (m)	20	20
x_0 (m)	-20	-20
T (s)	40	40

the values for x_0 also deviate between Table S3 and Table 1 in Section 2. This is due to a shift in the coordinate system. XBeach is a coastal model that defines the seaside at its origin, as opposed to the riverside as the origin of the Metronome coordinate system. Accordingly, for XBeach implementation, we subtract the flume length (L) and width for each x-coordinate and y-coordinate, respectively. This implies that for the XBeach coordinate system, the origin of $(x_0, y_0) = (0, 0)$ shifts to $(x_0, y_0) = (-20, -3)$, with coordinates in m.

In the momentum equations (Eqs. S2-S3) in the x and y directions, additional inertial terms associated with the accelerating reference frame (Metronome tilting) would, in principle, appear on the right-hand side. However, these contributions are neglected, as their magnitude is much smaller than gravitational acceleration set at $g = 9.81\ \mathrm{m/s^2}$. Specifically, the maximum tilting acceleration,

$$a_{\text{tilt,max}} = a_1\left(\frac{2\pi}{T}\right)^2 \approx 0.0018\ \mathrm{m/s^2} \text{ (for symmetric tilt) and } 0.0033\ \mathrm{m/s^2} \text{ (for asymmetric tilt)} \ll g = 9.81\,\mathrm{m/s^2}$$

See also Fig. S21.c for the second tilt derivative at $x = 0$ m, which is where the maximum acceleration effects occur. Consequently, the momentum equations reduce to the standard depth-averaged shallow water form.

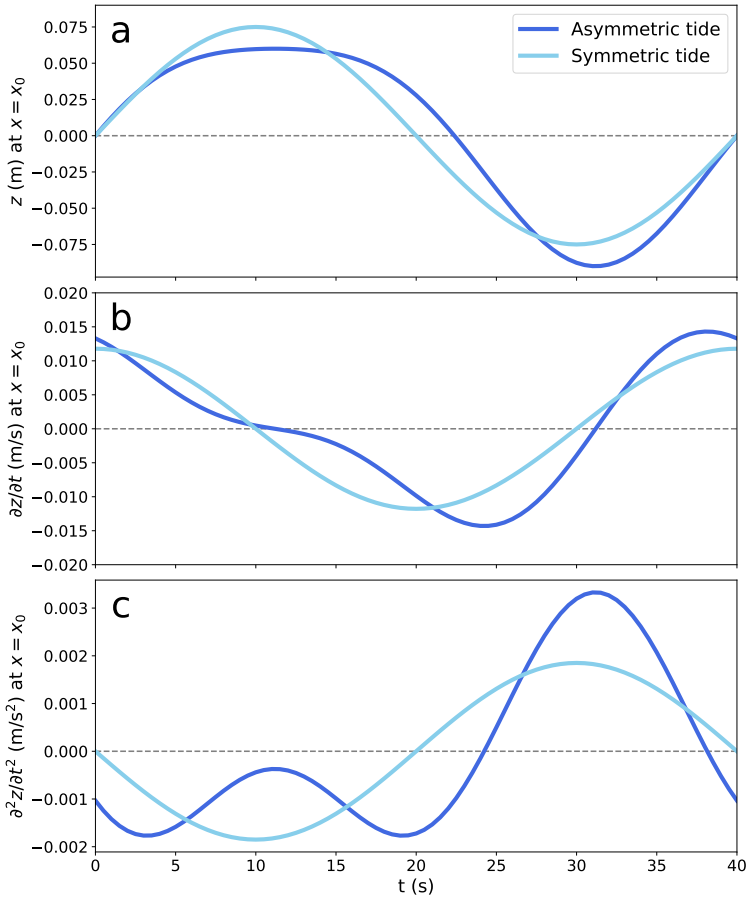

Figure S21. Metronome tilt position and its derivatives at $x = 0$ m (in XBeach $x = -20$ m) during a single emulated tidal cycle for the two different tidal settings in the dataset (Table S3). (a) Position z (Eq. 1; Section 2). (b) First derivative $\partial z/\partial t$ (right side of Eq. S5). (c) Second derivative $\partial^2 z/\partial t^2$.

References

Kleinhans, M., Baltussen, S., Nota, E., Cox, J., Meijer, H., and Hugtenburg, J.: Allowing Natural Sedimentation in the Nieuwe Waterweg to Reduce Salinity Intrusion and the Effects of Sea Level Rise, Blue Pap., 5, 24–34, https://doi.org/10.58981/bluepapers.2026.1.11, 2026.

McCall, R., Quataert, E., Roelvink, D., van Dongeren, A., de Bakker, A., de Ridder, M., de Goede, R., de Vet, L., and van der Lugt, M.: XBeach Documentation, Release BOI-Phase3-5956, 2022.

Nota, E. W., van Amstel, B. A., Nijland, W., van Maarseveen, M. C., and Kleinhans, M. G.: Data supplement to "Remote sensing of a gantry-equipped facility: optimizing accuracy by integrating SfM photogrammetry and laserscan computer graphics through fixed base model geometry" [Dataset], Yoda - Utrecht Univ., https://doi.org/10.24416/UU01-SGM22N, 2025.

Nota, E. W., Li, Y., Beyaard, L., Upson, M., Wagenaar, M. L., Nassralla, Z., Baltussen, S. J., van Amelsfort, E., Gubbels, L. M., Leahy, D., Muller, J. J., van Amstel, B. A., Donders, J. J., Rossius, J.-E., van Maarseveen, M. C., Markies, H., van Eijk, A. M., van Dam, B. D.,

Nussbaum, M., Faraji Gargari, S., Brunst, V., Braat, L., and Kleinhans, M. G.: Data supplement to "Experimental dataset on estuarine hydrodynamics and morphodynamics for various planforms and timescales" [Dataset], Yoda - Utrecht Univ., https://doi.org/10.24416/UU01-KKEUY5, 2026a.

Nota, E. W., Nussbaum, M., Upson, M., Leahy, D., Langenbach, J.-W. H., and Kleinhans, M. G.: Quantitative water depth determination in large experimental timeseries through combining spectrophotometry and machine learning, ESS Open Arch., https://doi.org/10.22541/essoar.177082648.88604562/v1, 2026b.

Nota, E. W., Nussbaum, M., Upson, M., Leahy, D., Langenbach, J.-W. H., and Kleinhans, M. G.: Data supplement to "Quantitative water depth determination in large experimental timeseries through combining spectrophotometry and machine learning" [Dataset], Yoda - Utrecht Univ., https://doi.org/10.24416/UU01-2XBVKK, 2026c.

Nota, E. W., van Amstel, B. A., Nijland, W., van Maarseveen, M. C., and Kleinhans, M. G.: Remote sensing of a gantry-equipped facility: optimizing accuracy by integrating SfM photogrammetry and laserscan computer graphics through fixed base model geometry, Int. J. Appl. Earth Obs. Geoinf., 146, 15 098, https://doi.org/10.1016/j.jag.2026.105098, 2026d.

Roelvink, D., Reniers, A., Van Dongeren, A., De Vries, J. V. T., McCall, R., and Lescinski, J.: Modelling storm impacts on beaches, dunes and barrier islands, Coastal Eng., 56, 1133–1152, https://doi.org/10.1016/j.coastaleng.2009.08.006, 2009.

Roelvink, D., Reniers, A., Van Dongeren, A., Van Thiel de Vries, J., Lescinski, J., and McCall, R.: XBeach model description and manual, 2010.

Smit, P., Stelling, G., Roelvink, J., Van Thiel de Vries, J., McCall, R., Van Dongeren, A., Zwinkels, C., and Jacobs, R.: XBeach: Non-hydrostatic model: Validation, verification and model description, Delft Univ. Technol, 59, https://oss.deltares.nl/documents/4142077/4199062/non-hydrostatic_report_draft.pdf/eadc1aff-6e19-6e82-2747-3c11c30457ee?t=1624871720408, 2010.

Van de Lageweg, W. I., van Dijk, W. M., Box, D., and Kleinhans, M. G.: Archimetrics: a quantitative tool to predict three-dimensional meander belt sandbody heterogeneity, Depositional Rec., 2, 22–46, https://doi.org/10.1002/dep2.12, 2016.

Van Dijk, W. M., Van de Lageweg, W., and Kleinhans, M. G.: Experimental meandering river with chute cutoffs, J. Geophys. Res.: Earth Surf., 117, https://doi.org/10.1029/2011JF002314, 2012.